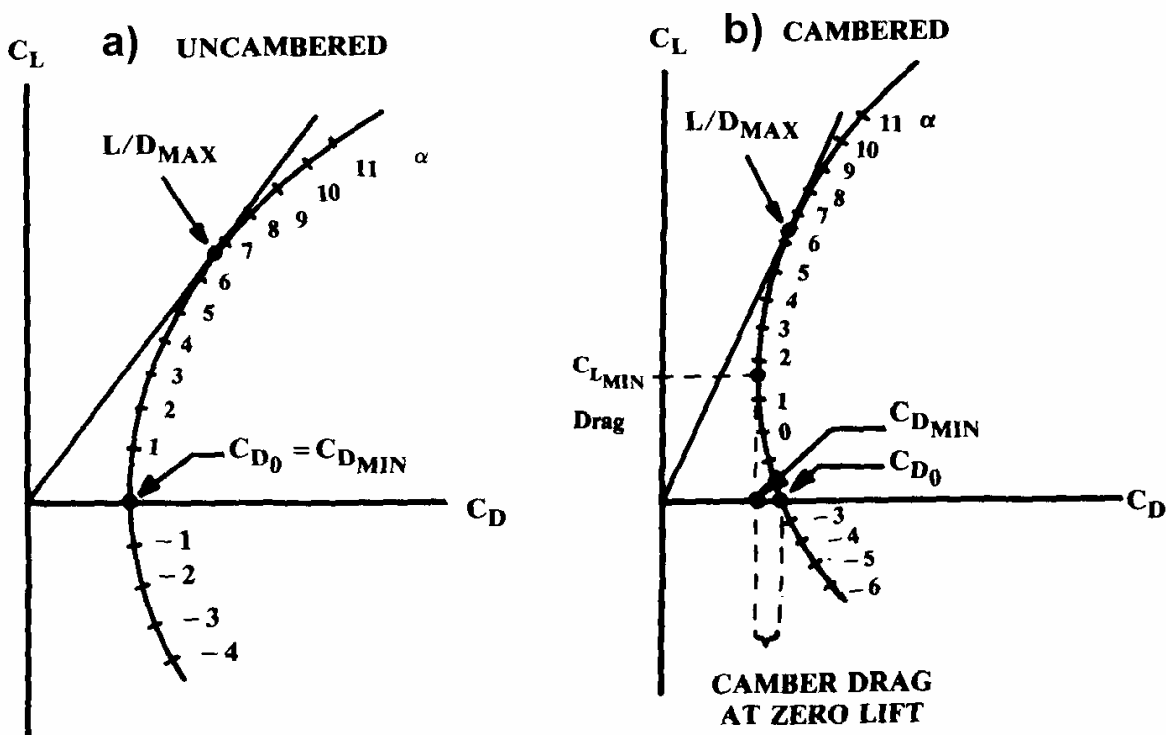


# 13 Drag Prediction

## 13.1 Drag Polar

In Section 2 under Step 14 it was a requirement that the flight performance has to be checked to complete the aircraft design process. This is only possible if the drag polar that forms the starting point for checking the flight performance is known. The polar creates the connection between lift and drag (Fig. 13.1). When determining the polar, the main task is to calculate the drag: the required lift is predefined, as a rule (in cruise flight, for example, due to the fact that lift equals the aircraft's weight).



**Fig. 13.1** The polar for uncambered and cambered airfoils. The angle of attack  $\alpha$  for  $C_D = f(C_L)$  is also indicated on the polar

If the polar is stated as an equation, the drag coefficient is written as a function of the lift coefficient. A polar for an uncambered airfoil as in Fig. 13.1 can be written in the following form:

$$C_D = C_{D0} + k \cdot C_L^2 \quad . \quad (13.1)$$

wherein

$$k = \frac{1}{\pi \cdot A \cdot e} \quad (13.2)$$

with the Oswald factor  $e$  and the aspect ratio  $A$ . Here the effective aspect ratio  $A_{\text{eff}}$  according to Section 7 should be used for the aspect ratio  $A$ , in order to take account of the influence of endplates or winglets, which increase the effective aspect ratio  $A_{\text{eff}}$  compared to the aspect ratio calculated with  $A = b^2/S$ . Irrespective of which aspect ratio is included in the calculation, the symbol  $A$  is simply retained in the equations in this case. The final result is

$$C_D = C_{D0} + \frac{C_L^2}{\pi \cdot A \cdot e} . \quad (13.3)$$

A polar for an uncambered airfoil as in Fig. 13.1 can be written in the following form:

$$C_D = C_{D,\min} + k(C_L - C_{L,\min})^2 . \quad (13.4a)$$

- In the case of an *uncambered airfoil* the drag is minimal if the lift is zero. This is the case with an angle of attack of  $\alpha = 0$ .
- In the case of a *cambered airfoil* the drag is minimal for a specific positive lift. This shifts the polar upward. For airfoils with a small camber this shift is minimal. For this reason, a polar according to equation (13.3) can be used for simplification.
- In the case of *high angles of attack* close to the maximum angle of attack  $\alpha_{C_{L,\max}}$ , the drag increases more sharply than in the parabolic form according to equations (13.3) and (13.4). A formulation with a term  $(C_L - C_{L,\min})^4$  is able to represent the correct drag coefficients for both low and high lift coefficients:

$$C_D = C_{D,\min} + k_1(C_L - C_{L,\min})^2 + k_2(C_L - C_{L,\min})^4 . \quad (13.4b)$$

In the further course of this section only the simple description of the polar according to equation (13.3) will be used.

## 13.2 Drag

The drag can be classified according to physical causes or according to the drag-inducing elements.

## Classification of drag according to physical causes

The *total drag* can be subdivided into (compare with Equation 13.3):

1. *zero-lift drag*: drag without the presents of lift;
2. *induced drag*: drag due to lift.

In addition *wave drag* comes into play, caused by a Mach number  $M$  that is greater than the critical Mach number  $M_{crit}$ . By definition,  $M_{crit}$  is the flight Mach number where a flow Mach number  $M = 1$  arises locally on the aircraft for the first time with increasing airspeed. This can, for example, occur on top of the wing. Chapter 7 gives more information on this phenomenon.

Very varied suggestions are made in the literature to further classify drag. One version (see Fig. 13.2) subdivides the zero-lift drag into *profile drag*, *interference drag*, and *miscellaneous drag* (*trim drag* and *additional or parasite drag*). The profile drag can in turn be subdivided into *skin-friction drag* and *pressure drag*.

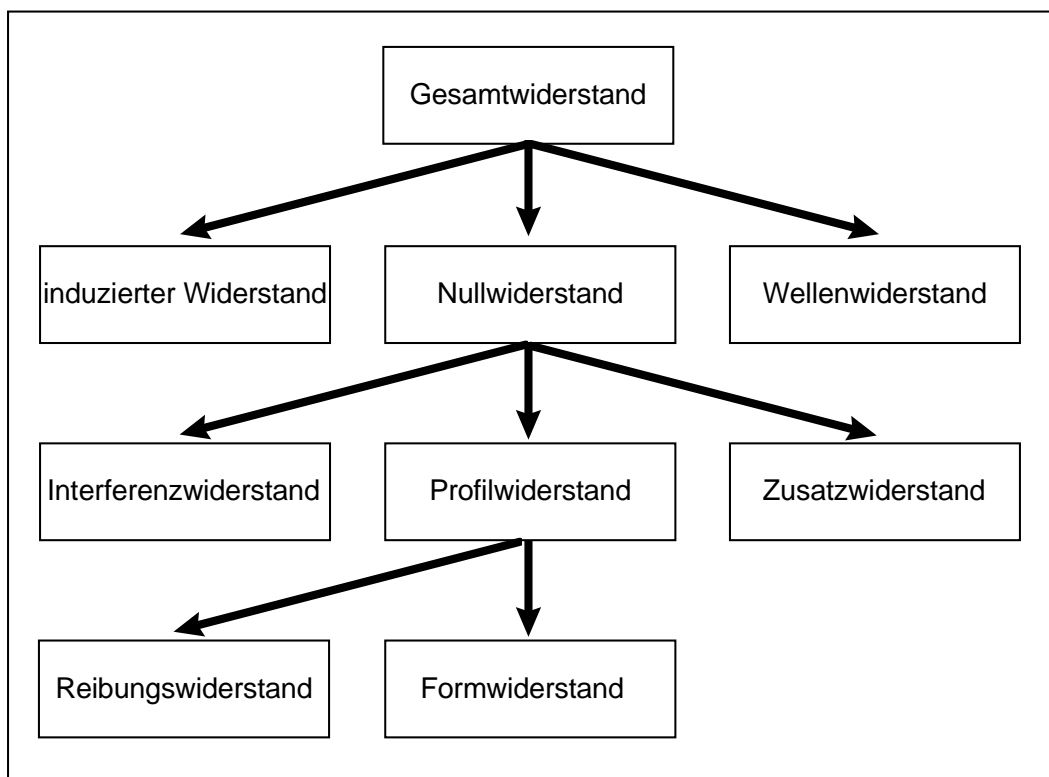


**Fig. 13.2** One of several possibilities to subdivide drag

- **Wave drag** is caused by shock waves on the airfoil. At high Mach numbers, both the zero-lift drag and the induced drag are increased by wave drag. The wave drag is only shown if it is calculated separately (and not as part of zero-lift drag and induced drag).
- **Skin-friction drag** is caused by the shear flow in the thin boundary layer close to the airfoil surface.

- **Form drag** is dependent upon the boundary layer, which can assume a large thickness especially in areas of separated flow and therefore prevents pressure being regained in the area of the trailing edge.
- **Interference drag** is caused by the mutual influence of the flow around neighboring components. The closer two components are, the greater the interference drag.
- **Trim drag** is caused by the elevator or horizontal stabilizer being deflected to retain the equilibrium around the lateral axis, and lift or negative lift being created on the horizontal tailplane. This results in a change in the induced drag on the horizontal tailplane and on the wing. This change in drag can be individually recorded on the wing and on the horizontal tailplane, but is sometimes also calculated separately and shown as trim drag.
- **Additional drag** (parasite drag) refers to drag components that tend to be recorded approximately and generally. The term "additional drag" is used, for example, with reference to drag caused by:
  - flaps and slats;
  - landing gear;
  - cockpit windows;
  - leakages in the pressurized fuselage.

## Classification of drag according to drag-inducing elements

In **Roskam VI**, for example, drag is calculated individually for the following elements:

- wing;
- fuselage;
- empennage;
- nacelle and pylon;
- flaps and slats;
- landing gear;
- cockpit windows;
- and other elements (lump-sum).

## Literature on calculating drag

This section contains key parameters and equations for calculating a simple polar for initial comparative studies and flight performance calculations. A selection of basic equations from **DATCOM 1978** is presented primarily for subsonic flow. It is important to bear in mind that **DATCOM 1978** was not actually created for detailed flight performance calculations, but rather only for calculating aircraft dynamics. In **DATCOM 1978** (Section 4.5.3.1) the following comment therefore appears:

*It should be pointed out that the basic approach taken here is satisfactory for preliminary design stability studies and that no attempt is made to provide methods suitable for performance estimates.*

Despite this statement, **DATCOM 1978** contains one of the most detailed publicly available handbook methods for calculating drag. The DATCOM version therefore also forms the basis for aircraft design in textbooks such as **Roskam VI** and **Raymer 1992**. **Hoerner 1965** is still a central source for answering further detailed questions on the subject of "drag".

## Significance of drag calculation in aircraft design

In a similar way to forecasting mass, forecasting aircraft drag is of considerable importance for the aircraft project. If it should transpire during flight testing that the aircraft drag is higher than assumed, it may be the case that the specified range of the aircraft cannot be complied with. This may lead to contractual penalties for aircraft which have already been ordered or even to orders being cancelled. Owing to the importance of forecasting aircraft drag, aircraft manufacturers have developed their own detailed computer-aided procedures, which are not accessible to the public. One in-house method that meanwhile appeared in public is **Boeing 1970**.

## Procedures for calculating drag

On a somewhat extended scale compared to equation (13.3), the polar is described here by

$$C_D = C_{D,0} + \Delta C_{D,flap} + \Delta C_{D,slat} + \Delta C_{D,gear} + \Delta C_{D,wave} + \frac{C_L^2}{\pi \cdot A \cdot e} . \quad (13.5)$$

In this version

$C_{D,0}$  is the zero-lift drag of the aircraft when the slats, landing flaps and landing gear are retracted (clean configuration). Their additional drag is taken into account separately by

$\Delta C_{D,flap}$ ,  $\Delta C_{D,slat}$ ,  $\Delta C_{D,gear}$  calculated according to Section 5. In addition,

$\Delta C_{D,wave}$  is the drag rise due to wave drag. A typical increase in drag with the Mach number is shown by Fig. 13.6 for four different types of aircraft. An estimation method is derived from Fig. 13.6 with equation (13.25).

$e = 0.7$  with **extended** flaps, slats and landing gear,

$e = 0.85$  can be used for **retracted** flaps, slats and landing gear for simplicity's sake. If one wishes to go further, a calculation of the Oswald factor  $e$  according to equation (13.26) is also possible.

### 13.3 Zero-lift Drag

Two methods are put forward to calculate the zero-lift drag of aircraft  $C_{D,0}$ :

1. Calculation of zero-lift drag from equivalent skin-friction drag (equivalent skin-friction method);
2. Calculation of zero-lift drag from the individual drag of components (component build-up method).

The first version is simpler and generally less precise, as details of the flow phenomena are not incorporated in the method.

#### **Calculating the zero-lift drag coefficient $C_{D,0}$ from the equivalent skin-friction drag coefficient $C_{fe}$**

This method uses the aircraft geometry which is now known according to the preceding design steps to estimate the zero-lift drag  $D_0$  with the aid of an equivalent skin-friction coefficient  $C_{fe}$ . The skin-friction coefficient multiplied by the dynamic pressure and the wetted area gives the zero-lift drag:  $D_0 = q C_{fe} S_{wet} = q C_{D,0} S_W$ . In contrast to the skin-friction drag coefficient  $C_f$ , the equivalent skin-friction coefficient  $C_{fe}$  also takes into account the other forms of drag contributing to the zero-lift drag; these are form drag, interference drag, trim drag and additional drag. The equivalent skin-friction coefficient  $C_{fe}$  is derived from measured values of the zero-lift drag. For this reason  $C_{fe}$  includes all drag contributions as mentioned.

$$C_{D,0} = C_{fe} \cdot \frac{S_{wet}}{S_W} . \quad (13.6)$$

Empirical values for  $C_{fe}$  are contained in Table 13.1 and Table 13.2.

$S_{wet}$  is the wetted area of the whole aircraft. In the case of conventional configurations the following parts must be taken into account, as a rule:

- fuselage;
- wings;
- horizontal and vertical tailplanes;
- nacelles and pylons.

$$S_{wet} = S_{wet,F} + S_{wet,W} + S_{wet,H} + S_{wet,V} + n_E \cdot S_{wet,N} + n_E \cdot S_{wet,pylons} . \quad (13.7)$$

In the case of unconventional configurations the wetted area of the aircraft has to be determined with the other corresponding components of the aircraft.

**Table 13.1** The equivalent skin-friction drag coefficient  $C_{fe}$  on the basis of general experience (Roskam I)

aircraft type	$C_{fe}$ - subsonic
jets	0.003 ... 0.004
twins	0.004 ... 0.007
singles	0.005 ... 0.007
sailplane	0.003

The drag calculation with the equivalent skin-friction coefficient  $C_{fe}$  is thus reduced to the determination of the wetted areas.

**Table 13.2** The equivalent skin-friction drag coefficient  $C_{fe}$  on the basis of general experience (Raymer 1992)

aircraft type	$C_{D_0} = C_{fe} \frac{S_{wet}}{S_{ref}}$	$C_{fe}$ -subsonic
Bomber and civil transport		0.0030
Military cargo (high upsweep fuselage)		0.0035
Air Force fighter		0.0035
Navy fighter		0.0040
Clean supersonic cruise aircraft		0.0025
Light aircraft – single engine		0.0055
Light aircraft – twin engine		0.0045
Prop seaplane		0.0065
Jet seaplane		0.0040

The **wetted area of fuselages with a cylindrical middle section** is as follows for  $\lambda_F \geq 4.5$  according to Torenbeek 1988:

$$S_{wet,F} = \pi \cdot d_F \cdot l_F \cdot \left(1 - \frac{2}{\lambda_F}\right)^{2/3} \left(1 + \frac{1}{\lambda_F^2}\right) \quad (13.8)$$

$d_F$  Fuselage diameter. For non-circular fuselages  $D_F$  is calculated from the fuselage circumference  $P$  with  $d_F = P / \pi$

$\lambda_F$  Fuselage fineness ratio,  $\lambda_F = l_F / d_F$ .

The **wetted area of streamlined fuselages** without the cylindrical middle section is as follows according to **Torenbeek 1988**:

$$S_{wet,F} = \pi \cdot d_F \cdot l_F \cdot \left( 0.5 + 0.135 \cdot \frac{l_n}{l_F} \right)^{2/3} \left( 1.015 + \frac{0.3}{\lambda_F^{1.5}} \right) \quad (13.9)$$

$l_n$  The distance from the aircraft nose in x direction to the start of the cylindrical part of the fuselage.

The **wetted area of the wing** is as follows according to **Torenbeek 1988**:

$$S_{wet,W} = 2 \cdot S_{exp} \cdot \left( 1 + 0.25 \cdot (t/c)_r \cdot \frac{1 + \tau \cdot \lambda}{1 + \lambda} \right) \quad (13.10)$$

$S_{exp}$  Exposed wing area (without the part of the wing area  $S_w$  running through the fuselage).

$\tau$  Ratio of relative airfoil thicknesses, wing tip/wing root,  $\tau = (t/c)_t / (t/c)_r$

$\lambda$  Taper,  $\lambda = c_t / c_r$ .

Equation (13.8) can also be applied to the horizontal and vertical tailplane or the canard.

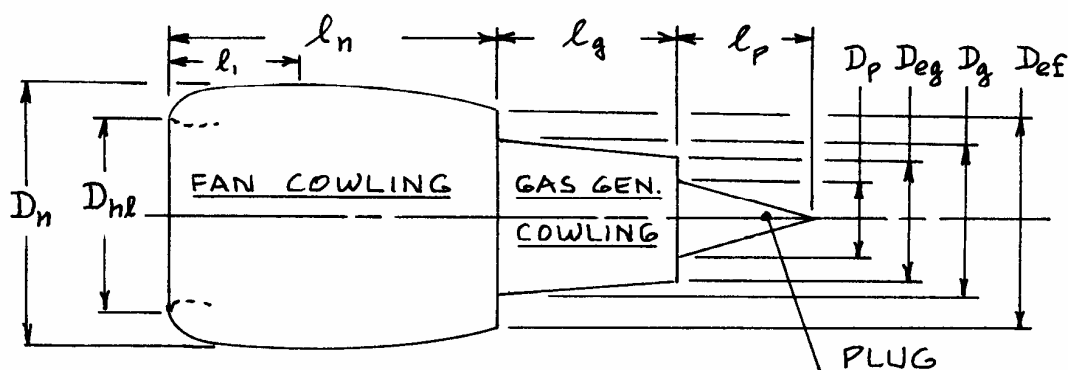


**Fig. 13.3** Geometry of a nacelle as used for the calculation of its wetted area. The distance  $l_1$  is measured from the leading edge to the position of maximum thickness of the fan cowling

The **wetted area of a nacelle** is as follows according to **Torenbeek 1988** with the geometrical parameters from Fig. 13.3:

$$S_{wet,N} = S_{wet,fan\ cowl.} + S_{wet,gas\ gen.} + S_{wet,plug} \quad (13.11)$$

$$S_{wet,fan\ cowl.} = l_n \cdot D_n \cdot \left[ 2 + 0.35 \frac{l_1}{l_n} + 0.8 \cdot \frac{l_1 \cdot D_{hl}}{l_n \cdot D_n} + 1.15 \cdot \left( 1 - \frac{l_1}{l_n} \right) \cdot \frac{D_{ef}}{D_n} \right] \quad (13.12)$$

$$S_{wet,gas\ gen.} = \pi \cdot l_g \cdot D_g \cdot \left[ 1 - \frac{1}{3} \cdot \left( 1 - \frac{D_{eg}}{D_g} \right) \cdot \left( 1 - 0.18 \cdot \left( \frac{D_g}{l_g} \right)^{\frac{5}{3}} \right) \right] \quad (13.13)$$

$$S_{wet,plug} = 0.7 \cdot \pi \cdot l_p \cdot D_p \quad (13.14)$$

A simple approximation formula should be found for the **wetted area of the pylon**  $S_{wet,pylons}$  according to the geometry.

### Calculation of the zero-lift drag coefficient $C_{D,0}$ from the individual drag of components

When calculating the polar from the individual drag of components (component build-up method), the zero-lift drag is calculated separately for each component. For simplification, the induced drag can be determined as in Section 5 with the aid of an assumed Oswald factor  $e$ .

The **zero-lift drag** of each component derives from:

1. the **skin friction drag coefficient**  $C_f$ ;
2. a **form factor**  $FF$ , which takes into account the pressure drag of the component;
3. an **interference factor**  $Q$ , which takes into account the interference drag;
4. the factor  $S_{wet} / S_{ref}$ , which serves to relate the drag coefficient of the component to the reference wing area.

Thus, the zero-lift drag would then be

$$C_{D0} = \sum_{c=1}^n C_{f,c} \cdot FF_c \cdot Q_c \cdot \frac{S_{wet,c}}{S_{ref}} \quad .$$

This takes account of the individual drag of all  $n$  components (referred to as "c"). However, the zero-lift drag of some components and some effects are difficult to deal with in the way described above. Therefore two terms are added to the above equation. It is then

$$C_{D0} = \sum_{c=1}^n C_{f,c} \cdot FF_c \cdot Q_c \cdot \frac{S_{wet,c}}{S_{ref}} + C_{D,misc} + C_{D,L+P} . \quad (13.15)$$

$C_{D,misc}$  contains the zero-lift drag of all other components, such as the landing gear.  $C_{D,L+P}$  represents all the additional drag due to leakages in the pressure cabin, e.g. at doors, and smaller drag, e.g. caused by aerials.

**Re 1.)** The **skin-friction coefficient**  $C_f$  describes the drag of a longitudinal flow along a flat plate. In the case of *laminar flow* the following applies:

$$C_{f,laminar} = 1.328 / \sqrt{\text{Re}} . \quad (13.16)$$

In the case of *turbulent flow* the skin-friction drag according to **DATCOM 1978** (4.1.5.1-26) and **Raymer 1992** equation (12.27) is

$$C_{f,turbulent} = \frac{0.455}{(\log \text{Re})^{2.58} \cdot (1 + 0.144 \cdot M^2)^{0.65}} . \quad (13.17)$$

Equation (3.17) is illustrated in Fig. 13.4. The Reynold's number is known to be

$$\text{Re} = \frac{V \cdot l}{v} . \quad (13.18)$$

In the case of a wing or empennage, the characteristic length  $l$  is the mean aerodynamic chord (MAC). In the case of the fuselage, the characteristic length is the total length of the fuselage.  $v$  is the kinematic viscosity, which is a function of aircraft altitude.

If the surface is relatively rough, the skin-friction drag  $C_{f,turbulent}$  will be higher than calculated by equation (13.16). This effect is taken account of according to **DATCOM 1978** (4.1.5.1-27) and **Raymer 1992** by means of a so-called *cut-off Reynold's number* (Fig. 13.5):

$$\text{für } M < 0.9: \quad \text{Re}_{\text{cut-off}} = 38.21 \cdot \left( \frac{l}{k} \right)^{1.053} , \quad (13.19)$$

$$\text{für } M \geq 0.9: \quad \text{Re}_{\text{cut-off}} = 44.62 \cdot \left( \frac{l}{k} \right)^{1.053} \cdot M^{1.16} . \quad (13.20)$$

In this  $l$  is the characteristic length and  $k$  is the surface roughness according to Table 13.3.

For	$\frac{V \cdot l}{\nu} > Re_{cut-off}$	$C_{f,turbulent}$ is calculated with $Re = Re_{cut-off}$ ,
for	$\frac{V \cdot l}{\nu} \leq Re_{cut-off}$	$C_{f,turbulent}$ is calculated with $Re = \frac{V \cdot l}{\nu}$ .

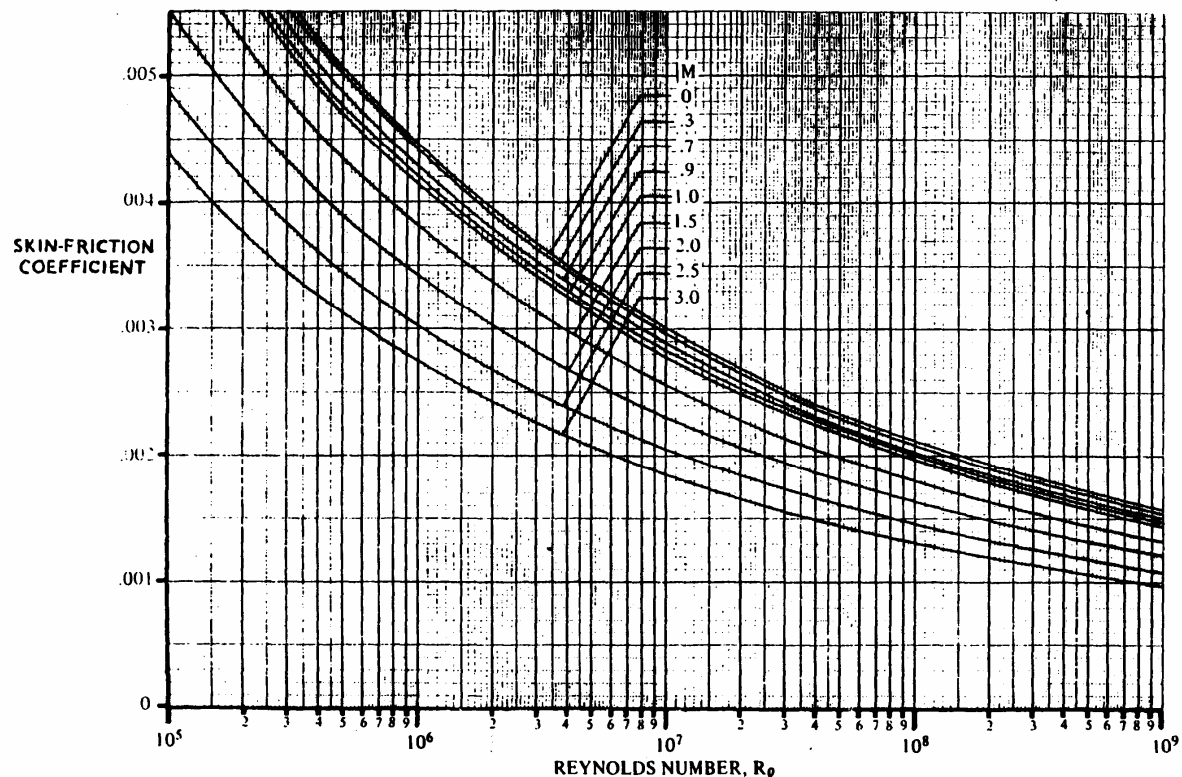


**Fig. 13.4** Skin-friction coefficient for turbulent flow DATCOM 1978 (4.1.5.1-26)

**Table 13.3** Surface-roughness height  $k$  from DATCOM 1978 (4.1.5.1-A)

Type of Surface	$k$ [mm]
aerodynamically smooth	0,00000
polished metal	0,00127
natural sheet metal	0,00406
smooth paint	0,00635
camouflage paint	0,01016

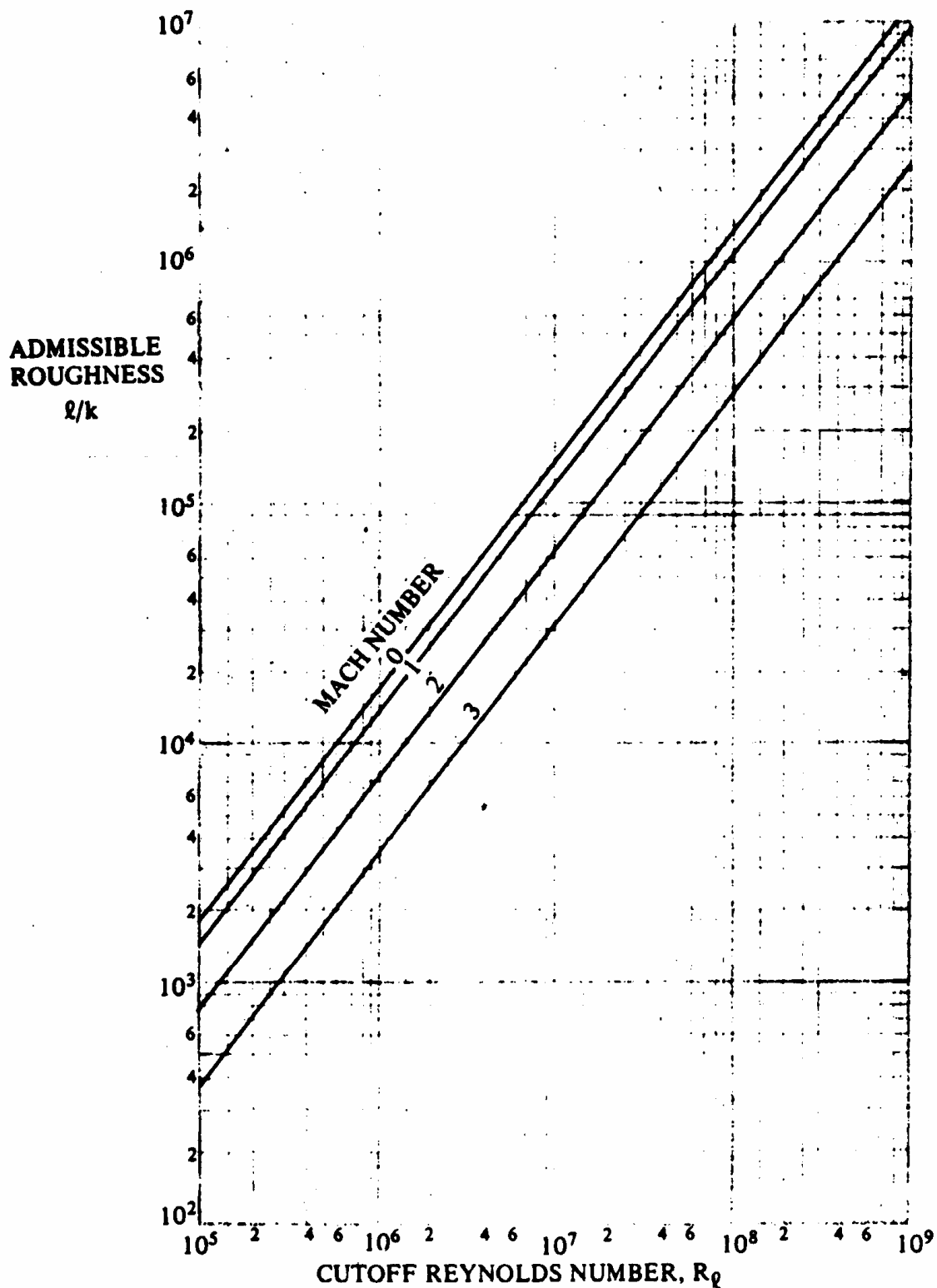


Bild 13.5

"Cutoff Reynolds Number" from DATCOM 1978 (4.1.5.1-26)

In the case of most aircraft the flow over the total wetted surface of the fuselage is turbulent. Laminar flow may exist on the front 10% to 20% of the wing. A carefully designed composite aircraft, such as the Piaggio GP 180, may exhibit laminar flow over 50% of the wing and over

20% to 35% of the fuselage. **Raymer 1992** suggests estimating the proportion of laminar flow  $k_{laminar}$  for the aircraft in question, in order to thus calculate a mean skin-friction drag

$$C_f = k_{laminar} \cdot C_{f,laminar} + (1 - k_{laminar}) \cdot C_{f,turbulent} . \quad (13.21)$$

**Re 2.)** The **form factor**  $FF$  is designated  $FF_w$  for *wings* and  $FF_h$  or  $FF_v$  for *empennages*. According to **DATCOM 1978** (4.1.5.1) – in a notation pursuant to **Raymer 1992** – the form factor is

$$FF = \left[ 1 + \frac{0.6}{x_t} \left( \frac{t}{c} \right) + 100 \left( \frac{t}{c} \right)^4 \right] \cdot \left[ 1.34 \cdot M^{0.18} \cdot (\cos \varphi_m)^{0.28} \right] . \quad (13.22)$$

$x_t$  is the position of maximum thickness according to Fig. 7.2.  $\varphi_m$  is the sweep angle of the %-line of maximum relative thickness.

According to **DATCOM 1978** (4.2.3.1) the form factor for the *fuselage* is calculated according to

$$FF_F = 1 + \frac{60}{\left( l_F / d_F \right)^3} + \frac{\left( l_F / d_F \right)}{400} . \quad (13.23)$$

According to **RAYMER 1992** the form factor for *nacelles* is calculated from

$$FF_N = 1 + \frac{0.35}{\left( l_N / d_N \right)} . \quad (13.24)$$

$l_N$  and  $d_N$  are the length and the diameter of the nacelle respectively.

**Re 3.)** The **interference factor**  $Q$  is selected according to Table 13.4.

No interference factor is given for the fuselage, because the interference of the components of a conventional aircraft design exists with the fuselage. On the other hand, the fuselage does not exhibit any interference with itself!

**Table 13.4** Interference factor  $Q$ 

Interference factor with respect to ...	Property	Interference factor $Q$
nacelle	engine mounted directly on the wing or fuselage	1.5
	distance of engine to wing respectively fuselage is smaller than engine diameter $d_N$	1.3
	distance of engine to wing respectively fuselage is greater than engine diameter $d_N$	1.0
wing	high-wing, mid-wing or low-wing position <i>with</i> aerodynamically optimized wing-fuselage fairing	1.0
	low-wing position <i>without</i> aerodynamically optimized wing-fuselage fairing	1.10 ... 1.40
fuselage	-	1.0
horizontal or vertical tailplane	conventional empennage	1.04
	H-tail	1.08
	V-tail	1.03

## 13.4 Wave drag

In this section an attempt is to be made to estimate the wave drag  $\Delta C_{D,wave}$ . As the flow configurations approaching sonic speed cannot be ascertained by using simple methods, we shall work on the basis of measured wave drag  $\Delta C_{D,wave}$  and try to generalize these measurements somewhat. A glance at Fig. 13.6 shows that the drag increase can be expressed by an equation in the following form:

$$\Delta C_{D,wave} = a \cdot \left( \frac{M}{M_{crit}} - 1 \right)^b \quad (13.25)$$

$M_{crit}$  is the critical Mach number of the (project) aircraft to be examined. For  $a$  and  $b$  the values from Table 13.5 have to be inserted. Parameters  $a$  and  $b$  have been ascertained mathematically, with the aim of reproducing the curve from Fig. 13.6 as precisely as possible. To do this, the critical Mach number  $M_{crit}$  was read off directly from Fig. 13.6. It is connected to  $M_{DD}$  in a certain way – by definition the Mach number where the wave drag reaches a value of 0.002 or 20 drag counts.

**Table 13.5** Parameters used to calculate wave drag

aircraft	$M_{DD}$	$M_{crit}$	$a$	$b$
C-130H	0.64	0.48	0.0198	2.17
C-5A	0.79	0.55	0.1002	4.77
B727	0.88	0.70	0.1498	3.20
F-106	0.99	0.90	0.8250	2.61

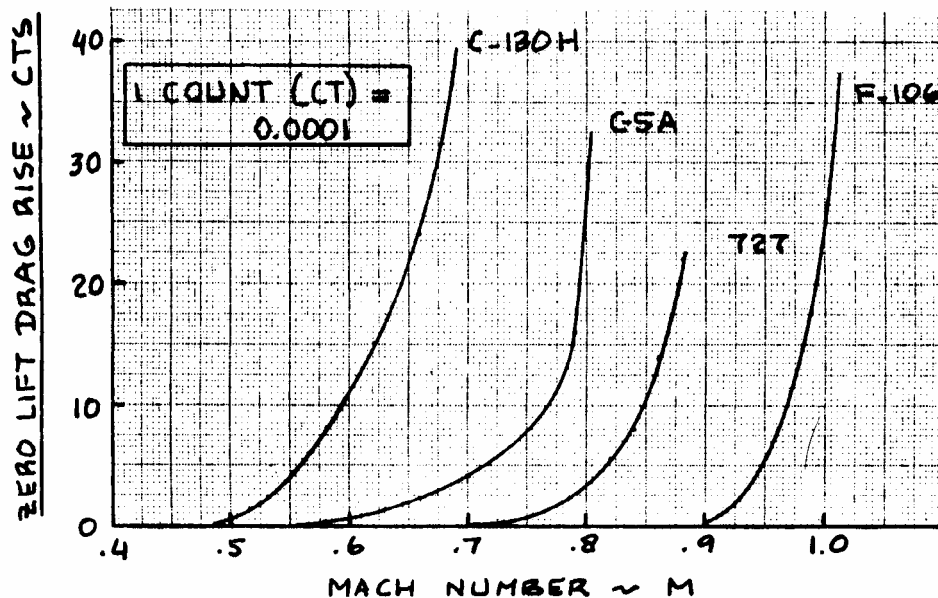
**Fig. 13.6** Drag rise due to wave drag for selected aircraft (Roskam II)

Fig. 13.6 contains data for the following aircraft:

- C-130H** Lockheed C-130H Hercules. Military transport, turboprop,  $m_{MTO} = 79000$  kg,  $V_{CR} = 167$  m/s.
- C-5A** Lockheed C-5A Galaxy. Military transport, jet,  $m_{MTO} = 349000$  kg,  $V_{CR} = 232$  m/s.
- 727** Boeing 727-200. Passenger aircraft, jet,  $m_{MTO} = 95000$  kg,  $V_{CR} = 254$  m/s,  $M = 0.82$ .
- F-106** Convair F-106A Delta Dart, the primary all-weather interceptor aircraft for the United States Air Force from the 1960s through the 1980s. Delta wing with NACA 0004-65 mod airfoil at root and tip. The fuselage was designed according to area ruling.

The practical procedure for estimating  $\Delta C_{D,wave}$  would therefore be as follows:

1. Select one of the four stated aircraft that looks as similar as possible to the project aircraft;
2. Determine  $M_{crit}$  of the project aircraft or estimate  $M_{crit}$  of the project aircraft from difference or ratio of  $M_{crit}$  and  $M_{DD}$  with the aid of Table 13.5. Note:  $M_{DD}$  of the project aircraft is known from the wing design;
3. Take parameters  $a$  and  $b$  from Table 13.6;
4. Estimate  $\Delta C_{D,wave}$  with the aid of equation (13.25) as a function of the Mach number.

## 13.5 Induced drag and Oswald factor

The Oswald factor  $e$  is required by equation (13.3) to calculate induced drag.

$$C_D = C_{D0} + C_{Di} = C_{D0} + \frac{C_L^2}{\pi \cdot A \cdot e} \quad (13.3)$$

According to **Howe 2000** (equation 6.14a), the Oswald factor  $e$  can be estimated for the subsonic range and for transonic flows ( $M < 0.95$ ) for aircraft with a wing aspect ratio of  $A > 5$  from

$$e = \frac{1}{(1+0.12 M^6) \left\{ 1 + \frac{0.142 + f(\lambda) A (10 t/c)^{0.33}}{(\cos \varphi_{25})^2} + \frac{0.1(3 N_e + 1)}{(4+A)^{0.8}} \right\}} . \quad (13.26)$$

In this equation

$M$  is the flight Mach number

$A$  is the (effective) aspect ratio

$t/c$  is the relative airfoil thickness

$\varphi_{25}$  is the wing sweep of the 25% line

$N_e$  is the number of engines **on** the wing (if none, then  $N_e = 0$ ).

$$f(\lambda) = 0.005 (1 + 1.5 (\lambda - 0.6)^2) . \quad (13.27)$$

In this equation  $\lambda$  is the wing taper. A typical value for  $f(\lambda)$  is 0.0062 .